Kyushu University Global COE Program
Journal of Novel Carbon Resource Sciences, Vol. 3, pp. 40-44, Feb. 2011

# Control of Morphology of Pt Nanoparticles and Pt-Pd Core-Shell Nanoparticles

Nguyen Viet Long[*1], Michitaka Ohtaki[*1], Masayuki Nogami[*2]

[*1]Faculty of Engineering Sciences, Kyushu University
[*2]Department of Materials Science and Engineering, Nagoya Institute of Technology

(Received December 20, 2010; accepted February 7, 2011)

In this paper, poly(vinylpyrrolidone) (PVP) protected Pt and Pt–Pd nanoparticles were synthesized by the reductions of $H_2PtCl_6$ and $Na_2PdCl_4$ in ethylene glycol (EG) using $AgNO_3$ as a structure–controlling agent. Transmission electron microscopy (TEM) and high resolution (HR)TEM were employed to study the morphology and size of Pt and Pt–Pd nanoparticles. The results showed that the size and morphology of Pt nanoparticle was precisely controlled by addition of $AgNO_3$. Accordingly, only under the selection of the appropriate chemicals and experimental conditions, Pt–Pd nanoparticles with their core–shell morphology were precisely controlled.

## 1. Introduction

In recent years, Pt and Pt–Pd nanoparticles have been intensively studied because of their excellent catalytic properties derived from their size and morphology[1,2]. It is known that characterizations of their sharp and polyhedral morphology of {111}, {100}, and {110} specific facets or planes, various sphere–like non–polyhedral morphologies as well as their defects need to be studied in detail. A more clear explanation is also necessary to clarify their catalytic and electrocatalytic features[1-3]. So far, new experimental observations in the surfaces of Pt nanoparticles have been highlighted. Specially, the special changes of its morphology under gas environment and pressure were studied[4,5]. In addition, the collapse in their structure and decline in catalytic activity are also discovered in the limit range of particle size <1 nm[6].

It is known that their catalytic and electrocatalytic characterizations originated from high surface–to–volume ratio and quantum size[7]. At present, the synergetic property between the layers of the core, the shell, and their interfaces in the core–shell configuration is of great interest. Recently, a comparison of catalytic property of single nanoparticles, bimetallic nanoparticles (various kinds of Pt–based alloys and core–shell structures), and Pt–based multi–composition catalysts has been carried out in detail[1-3,7]. Their improvements of catalytic activity and selectivity are expected to have a great impact in the realization of proton exchange membrane fuel cells (PEMFCs) with practical effective–cost design[1,2]. Therefore, the various methods to control the size and morphologies of nanoparticles have been proposed. Alternatively, the alloyed nanostructures were prepared[1-3]. As a result, their catalytic properties of Pt–based nanoparticles have been improved, but the precise control of the core–shell morphologies has shown to be a much more challenge. The metal shells commonly nucleate in the various random growth modes on the surfaces of other cores by self–aggregation and assembly during their chemical reduction[1,7]. Therefore, the chemical methods are considered as the feasible solutions to control the shells on the as–prepared and as–defined cores, which based on reducing two different metal salts to shape their core–shell configuration in the simultaneous or successive reductions of their salts. The different approaches utilize the chemical methods to design the shells on the cores by the simultaneous and successive reductions of their salts[1,2,7]. Accordingly, the microwave–heating technique was utilized for the fabrication of bimetallic Ag–Ni nanostructures[8].

In this research, the Pt cores were prepared by modified polyol method with the assistance of $AgNO_3$ as a structure–controlling agent. The facile polyol method was used to control the overgrowth of Pt–shell layers on the Pt–cores crystal surfaces. First, the previous reduction of $H_2PtCl_6$ by EG was carried out to make the Pt cores. Then, the successive reduction of $Na_2PdCl_4$ by EG was done to make the Pd shells. In the first section, Pt nanoparticles as the defined cores were formed in the homogeneous growth mode. Then, the Pd shells were formed in the slow reduction of $Na_2PdCl_4$ with EG. The epitaxial growth modes of Pd shells were found in the TEM and HRTEM evidences.

## 2. Experimental

### 2.1. Chemicals

Chemicals from Aldrich (or Sigma–Aldrich) were used in the experimental processes. They were polyvinylpyrrolidone (PVP, a protective reagent) (FW: 55,000), sodium tetrachloropalladate (II) hydrate ($Na_2PdCl_4$) (ACS reagent), and chloroplantinic acid hexahydrate ($H_2PtCl_6$) (ACS reagent) as precursors for producing Pt nanoparticles and Pt–Pd core–shell nanoparticles. Ethylene glycol (EG) was used as both the solvent and the reducing agent. Silver nitrate (metal basis) was used as a modifying agent. Solvents including ethanol, acetone, and hexane were used for washing and cleaning. Ionized, distilled, and mili–Q water were prepared by using a Narnstead nanopure $H_2O$ purification system. All chemicals used were of analytical grade and were used without any further purification.

### 2.2. Morphology control of Pt nanoparticles

In order to make Pt nanoparticles, 3 mL of EG, 1.5 mL of 0.0625 M $H_2PtCl_6$, 3 mL of 0.375 M PVP, and 0.5 mL of 0.04 M $AgNO_3$ were used. The volumes of 3 mL

EG and 0.5 mL 0.04 M $AgNO_3$ were mixed in a flask and heated to 160 °C. After the solution was mixed for 15 min, argon gas was bubbled for 20 min into the flask prior to the synthesis. The solution was refluxed for 2 h in an Ar gas atmosphere. Next, 30 μL of 0.0625 M $H_2PtCl_6$ was added to the flask at 160 °C, sequentially followed by the injection of 60 μL of 0.375 M PVP into the flask until 1.5 mL of 0.0625 M $H_2PtCl_6$ and 3 mL of 0.375 M PVP were added into the flask and reacted thoroughly under stirring for 15 min. The reduction of $H_2PtCl_6$ by EG occurred. The mixture was stirred in the flask at 160 °C for 15 min. As a result, a dark–brown solution containing Pt nanoparticles possess their polyhedral morphology.

### 2.3. Morphology control of Pt–Pd core–shell nanoparticles

At first, Pt nanoparticles were synthesized by the above stable and reliable procedure. Then, they were used as the as–prepared cores for producing the Pt–Pd core–shell nanoparticles. In a similar manner, 3 mL of EG and 0.5 mL of 0.04 M $AgNO_3$ were added to a flask, and the mixture was refluxed at 160 °C for 15 min. Then, 30 μL of 0.0625 M $Na_2PdCl_4$ was added in the flask, sequentially followed by the addition of 60 μL of 0.375 M PVP to the flask until 1.5 mL of 0.0625 M $Na_2PdCl_4$ and 3 mL of 0.375 M PVP were added and reacted thoroughly. The successive reduction of $Na_2PdCl_4$ by EG occurred under continuously stirring for 15 min. After that, the resultant mixture was kept in the flask while stirring it for 15 min. Next, the flask containing the product solution was moved out of the boiling–oil bath. In this process, the only formation of Pt–Pd core–shell nanoparticles was observed in the final product.

### 2.4. Characterization

To characterize the Pt nanoparticles and Pt–Pd core–shell nanoparticles, copper grids of containing Pt and Pt–Pd core–shell nanoparticles were maintained under vacuum by using a vacuum cabinet (JEOL–JEM–DSC10E Film Vacuum Desiccator Cabinet) prior to the TEM and HRTEM measurements. Then, the copper grids were treated again at the drying station (JEOL JDS–230F Drying Station). They were treated using an ion cleaner that employed the glow discharge in vacuum to remove any contamination (Ion Cleaner JIC–410 JEOL). The copper grids were maintained under conditions of very high vacuum in the transmission electron microscope (JEOL JEM–2100F or JEM–2010) overnight prior to the TEM and HRTEM measurements. The TEM images were obtained using a transmission electron microscope (JEOL JEM–2100F and JEM–2010) operated at 200 kV. For acquiring, visualizing, analyzing, and processing digital image data of Pt and Pt–Pd nanoparticles, DigitalMicrograph software (Gatan, Inc.) was used in our TEM and HRTEM studies.

## 3. Results and discussion

### 3.1. Size and morphology of Pt nanoparticles

Figure 1 showed TEM images of polyhedral Pt nanoparticles and polyhedral Pt nanoparticles of truncated polyhedral morphologies at the corners with the particle size of 8–18 nm by modified polyol method at 160 °C for 15 min using PVP and the structure–controlling agent of 0.04 M $AgNO_3$. There are more than 95% of Pt nanoparticles in the main forms of cubic, octahedral, and tetrahedral morphologies. In addition, their truncated cubic, octahedral, and tetrahedral morphologies were also observed. It is certain that the addition of $AgNO_3$ influenced on shaping the final morphology of Pt nanoparticles associated with their short synthetic time. The polyhedral Pt nanoparticles exhibit with three main kinds of cubic, octahedral, and tetrahedral Pt morphologies as well as their various truncated cubic, octahedral, and tetrahedral morphologies. The polyhedral morphologies show very sharp corners, edges, and facets. Typically, the sharp and polyhedral Pt nanoparticles of the characteristic low–index {100} and {111} planes or facets were considered in their practical applications in catalysis[1-3]. Therefore, a modified polyol with the assistance of $AgNO_3$ potentially offers the good ways to synthesize precious metal nanoparticles under their size and shape control[9]. For polyhedral Pt nanoparticles, it was observed that these Pt nanoparticles exhibiting the very good single–crystal structures were controlled in both the size and the morphology. In addition, some of twined Pt nanoparticles were also found. The results confirmed the polyhedral Pt nanoparticles in the homogenous single–crystal growth.

There are two main kinds of the nucleation and growth of metal nanoparticles[1,10,11] that consisted of various homogeneous and heterogeneous nucleations and growths. In our research, the homogeneous nucleation and growth become the preferential nucleation and growth. On the other hands, the heterogeneous nucleation and growth of Pt nanoparticles such as rods, wires, and flowers were difficult to observe. Here, the morphology of polyhedral Pt nanoparticles needs to be studied in the further details, especially their roles in the activity and selectivity in catalysis. In fact, the morphologies of quasi–sphere non–polyhedral Pt nanoparticles are very complicated both in the experimental TEM and HRTEM images and in their models[1-3]. The symmetry and regularity of the atomic arrangements on the surfaces of Pt nanoparticle in Figure 1 are very good in a single crystal structure and they are of the good morphologies of well–controlled Pt nanoparticles. It was observed that the average particle size of polyhedral Pt nanoparticles was approximately 10.24 nm in the nanosized range of 8–18 nm. Here the reduction of $H_2PtCl_4$ by EG occurred for the period about 15 to 20 min. The HRTEM images of single Pt nanoparticles (Figure 1(c)–(d)) showed the Pt lattice fringes with the inter–fringe distance ~0.230 nm close to the {111} planes showing Pt crystal of face–centered cubic (fcc) structure. However, the appearance of surface defects at their un–sharp corners. Therefore, they possess both the most characteristic low–index {100} and {111} planes in their polyhedral morphology. The surfaces of polyhedral Pt nanoparticles are the flat and sharp morphologies of better atomic arrangements. We proposed that the role of $Ag^+$ tends to direct the {100} and {111} selective growth modes of Pt nanoparticles leading

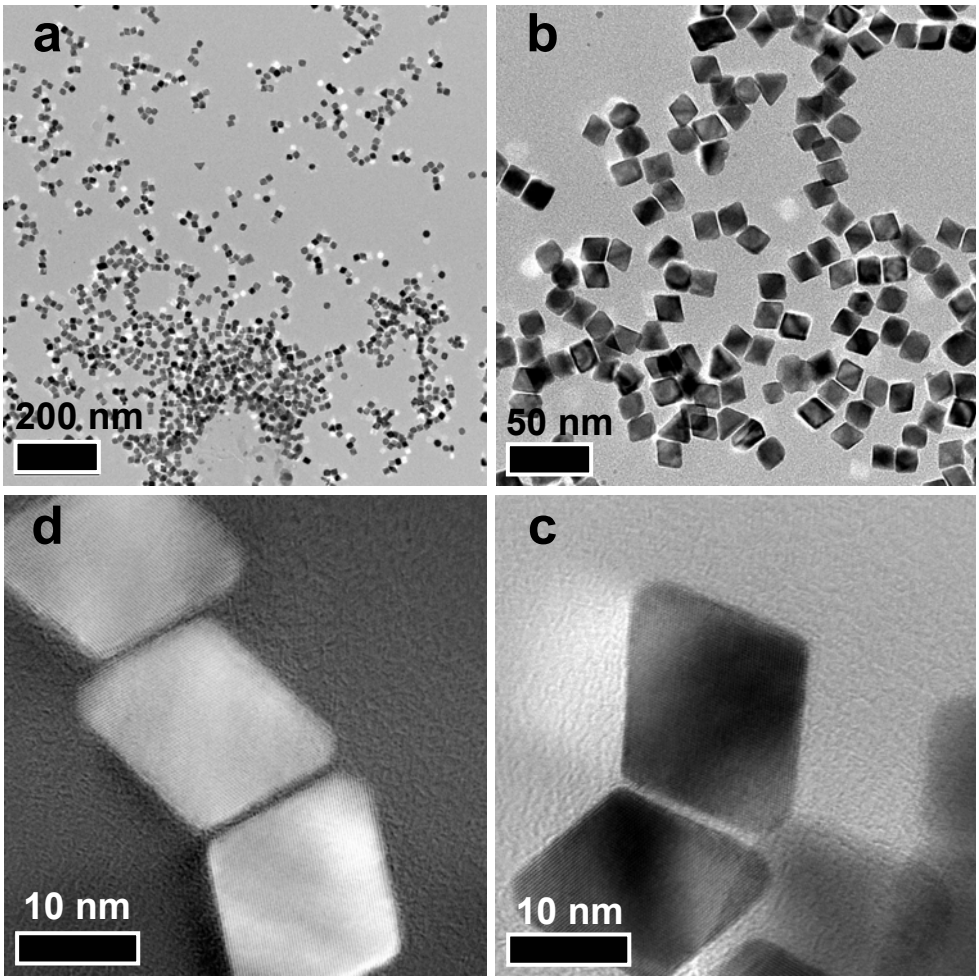


**Fig. 1** TEM and HRTEM images of polyhedral Pt nanoparticles. Their polyhedral morphologies with the truncated corners and surfaces are observed. Scale bars: (a) 200 nm; (b) 50 nm; (c)–(d) 10 nm.

to the formation of Pt nanoparticles with their polyhedral morphologies. However, the supply rates of polymer (PVP) and precursor ($H_2PtCl_6$), time and temperature are also very important to the appearance of polyhedral Pt nanoparticles. It was known that the role of $Ag^+$ enhances the {100} growth, and/or suppresses {111} growth and $Ag^+$ is reduced by EG at high temperature resulting in reduced silver species, such as $Ag_4^{2+}$ clusters and $Ag^0$ [9]. They are possibly adsorbed on the surface of {100} facets of Pt nanoparticles. They are removed by organic solvents, such as a mixture of ethanol and hexane. The illustrations of the formation of the terrace, ledge, and kinks of the particle surface were introduced[12], leading to form the positions of highly chemical reactivity due to their accessibility and coordinative un–saturation characterization.

### 3.2. Size and morphology of Pt–Pd core–shell nanoparticles

Figure 2 showed the Pt–Pd bimetallic nanoparticles of core–shell morphologies in the nanosized range of 16–25 nm based on the as–prepared Pt cores. So far, the methods of controlling metal core–shell have been difficult because of the alloying of two different metals[24,28]. For the common phenomena, the surface contacts between nanoparticles and bigger nanoparticles were established. This led to form the irregular and large particles[14]. It was clearly shown that there are two kinds of the metal–shell overgrowth that were the non–epitaxial growth mode and expitaxial growth mode of the metal–shell[1,2]. We can see that the morphologies of sharp corners and un–sharp corners with the round edges of Pt–Pd nanoparticles. This strongly depended on the resolution of microscopy (HRTEM) and its limitations. Most of Pt–Pd core–shell nanoparticles exhibited their polyhedral core–shell nanoparticles. Near–sphere Pt–Pd core–shell nanoparticle were also observed. The HRTEM images of the Pd–shell layers indicated that the Pd lattice fringes with the inter–fringe distance ~0.230 nm assigned to the distance between the {111} planes of face–centered cubic (fcc) Pd single crystal structure. In this case, it is certain that the effect of the synthetic approach using the assistance of $AgNO_3$ was confirmed in the sharp and polyhedral morphology control of these Pd–shell coatings. Based on the classical theory of nucleation and growth of single metal nanoparticles as well as the nucleation and growth of alloy and core–shell bimetal nanoparticles, the Gibbs free energy and overall excess free energy were considered in

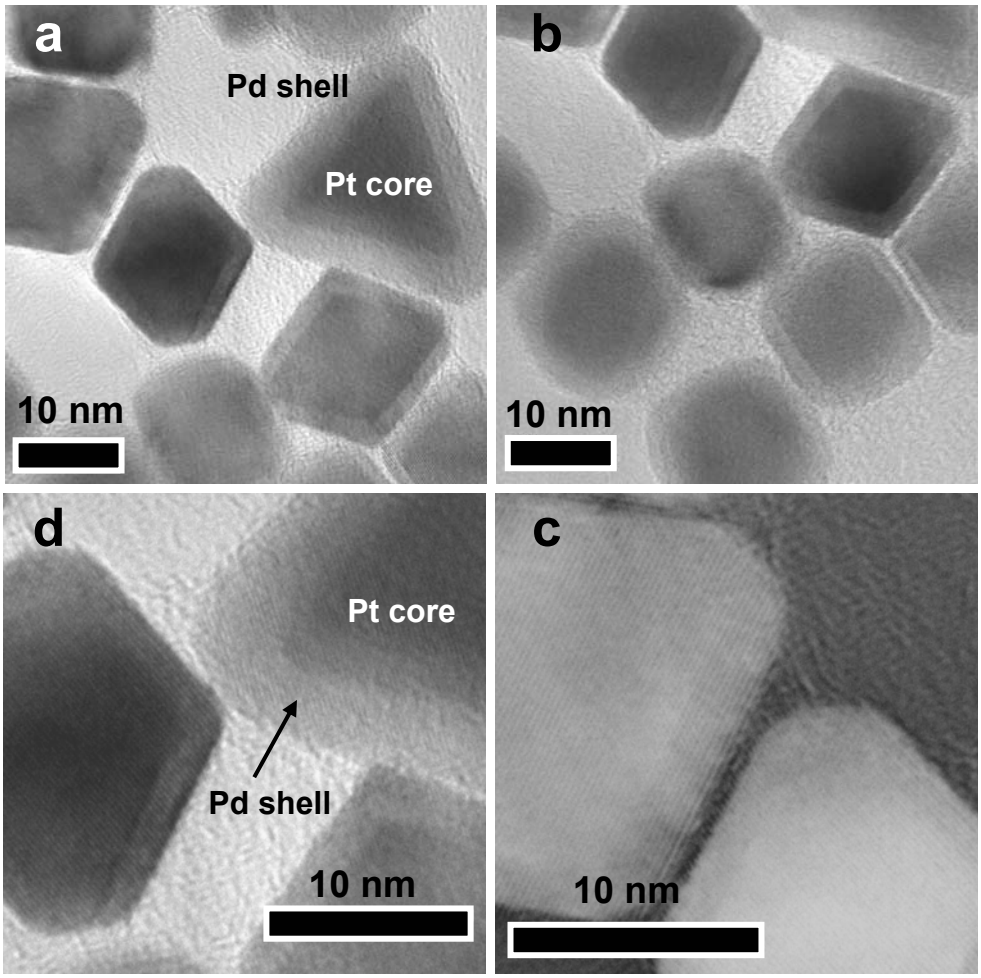


**Fig. 2** HRTEM images of Pt–Pd core–shell nanoparticles. Their polyhedral morphologies with the truncated corners and surfaces are observed. Scale bars: (a)–(d) 10 nm.

order to control their size and morphology for uniform formation of the core and/or the shell. In general, the Frank–van der Merwe (FM), Volmer–Weber (VW), and Stranski–Krastanov (SK) growth modes have explained the formation of various nanostructures of Pt–Pd based alloy, and Pt–based core–shell nanoparticles[1,2,14]. Figure 2 clearly showed the TEM and HRTEM images of the FM growth mode of the Pt–Pd core–shell nanoparticles. We suggested that the condition of the FM growth mode depended on the smooth surface of as–prepared polyhedral Pt nanoparticles, such as (111) facets. The Pd monolayers were described by the overgrowth from atomic monolayers according to the FM mode. In the HRTEM image of Figure 2(c)–(d), the layer–by–layer growth mode was observed in the shell–layer formation of Pt–Pd core–shell nanoparticle at their surfaces and corners. It was the oriented overgrowth of the single crystal Pd shell on the surface of the as–prepared Pt core that possessed a good lattice match. In addition, both Pt and Pd metals have the (fcc) crystal structure. Therefore, the Pd shell could grow epitaxially on the Pt core because of their same crystal structures. The thickness of the shell layer of 10 ± 1 Pd atomic monolayers was about 2.4 nm in Figure 2 (c)–(d). The overgrowths of atomic Pd monolayers of the Pt–Pd nanoparticles were formed in the FM growth mode. The results provided the experimental evidence phase segregation between the core (the as–prepared Pt nanoparticles) and the shell (the Pd shells). The thickness of Pd atomic monolayers or Pd shells was different from their surfaces of Pt nanoparticles. The directions of the overgrowth of atomic monolayers of metal shells were formed in both the FM and SK growth modes[1]. It was suggested that the attachments of small Pd nucleus (or very small Pd nanoclusters) were the common modes to form the Pd shells in the case of the slow reduction of $Na_2PdCl_4$ under control. They could deposit on the surfaces of Pt–core particles leading to their combination at their interfaces. This mechanism is possibly very good to make the core–shell structures in various ways of the very mild and slow reduction of metal ions for making the shell. It means that very small clusters will gradually deposit on the surfaces of as–prepared cores in the epitaxial growth modes (or both epitaxial and nonepitaxial overgrowth). Possibly, Pd nucleus or very small Pd nanoclusters of less than 1 nm deposited on the surfaces of Pt–Pd nanoparticles. The significantly structural changes of polyhedral Pt cores were not observed. At present, the great efforts are made to realize core–shell bimetallic

nanoparticles under size and morphology control. Only by varying the composition, reaction time and temperature, various kinds of metal precursors, polymers or ligands, reductants, and controlling reagents, the various sizes of layers of the shells and the cores can be precisely controlled.

## 4. Conclusions

In this study, Pt and Pt–Pd nanoparticles were synthesized by modified polyol method under size and morphology control. The evidences of the epitaxial overgrowth of the Pd–shell on the Pt–core due to the layer–by–layer mechanism were confirmed. In our results, we have suggested that the Pt–Pd core–shell nanoparticles were formed in both the Frank–van der Merwe (FM) layer–by–layer and Stranski–Krastanov (SK) island–on–wetting–layer growth modes. The Pt–Pd core–shell nanoparticles were observed in the SK and FM growth modes, respectively. However, the latter became a favorable growth mode in the formation of Pt–Pd core–shell nanoparticles.

References


1) Z. Peng, H. Yang, *Nano Today*, **4**, 143 (2009).
2) J. Chen, B. Lim, E. P. Lee, Y. Xia, *Nano Today*, **4**, 81 (2009).
3) M. Subhramannia, V. K. Pillai, *J. Mater. Chem.*, **18**, 5858 (2008).
4) M. Cabié, S. Giorgio, C. R. Henry, M. R. Axet, K. Philippot, B. Chaudret, *J. Phys. Chem. C*, **114**, 2160 (2010).
5) B. Lim, H. Kobayashi, P. Camargo, L. Allard, J. Liu, Y. Xia, *Nano. Res.*, **3**, 180 (2010).
6) Y. Sun, L. Zhuang, J. Lu, X. Hong, P. Liu, *J. Am. Chem. Soc.*, **129**, 15465 (2007).
7) N. Toshima, H. Yan, Y. Shiraishi, in *Metal nanoclusters in catalysis and materials science: The issue of size control*, eds. by B. Corain, G. Schmid, N. Toshima, Elsevier B.V., p.49 (2004).
8) M. Tsuji, S. Hikino, M. Matsunaga, Y. Sano, T. Hashizume, H. Kawazumi, *Mater. Lett.*, **64**, 1793, (2010).
9) H. Song, F. Kim, S. Connor, G. A. Somorjai, P. Yang, *J. Phys. Chem. B*, **109**, 188 (2005).
10) A. R. Tao, S. Hamas, P. Yang, *Small*, **4**, 310 (2008).
11) T. Sugimoto, in *Monodispersed particles*, eds. by T. Sugimoto, Elsevier, Amsterdam, p.187 (2001).
12) L. Y. Chang, A. S. Barnard, L. C. Gontard, R. E. Dunin–Borkowski, *Nano Lett.*, **10**, 3073 (2010).
13) R. Ferrando, J. Jellinek, R.L. Johnston, *Chem. Rev.*, **108**, 845 (2008).
14) L. Carbone, P. Cozzoli, *Nano Today*, **5**, 449 (2010).